Application of Trained POD-RBF to Interpolation in Heat Transfer and Fluid Mechanics

2018

Rebecca A. Ashley
University of Central Florida

APPLICATION OF TRAINED POD-RBF TO INTERPOLATION IN HEAT TRANSFER AND FLUID MECHANICS

by

REBECCA A. ASHLEY

A thesis submitted in partial fulfillment of the requirements
for the Honors in the Major Program in Mechanical Engineering
in the College of Engineering and Computer Science
and in the Burnett Honors College
at the University of Central Florida
Orland, Florida

Spring Term, 2018

Thesis Chair: Alain Kassab, PhD.

ABSTRACT

To accurately model or predict future operating conditions of a system in engineering or applied mechanics, it is necessary to understand its fundamental principles. These may be the material parameters, defining dimensional characteristics, or the boundary conditions. However, there are instances when there is little to no prior knowledge of the system properties or conditions, and consequently, the problem cannot be modeled accurately. It is therefore critical to define a method that can identify the desired characteristics of the current system without accumulating extensive computation time. This thesis formulates an inverse approach using proper orthogonal decomposition (POD) with an accompanying radial basis function (RBF) interpolation network. This method is capable of predicting the desired characteristics of a specimen even with little prior knowledge of the system. This thesis first develops a conductive heat transfer problem, and by using the truncated POD – RBF interpolation network, temperature values are predicted given a varying Biot number. Then, a simple bifurcation problem is modeled and solved for velocity profiles while changing the mass flow rate. This bifurcation problem provides the data and foundation for future research into the left ventricular assist device (LVAD) and implementation of POD – RBF.

The trained POD – RBF inverse approach defined in this thesis can be implemented in several applications of engineering and mechanics. It provides model reduction, error filtration, regularization and an improvement over previous analysis utilizing computational fluid dynamics (CFD).

DEDICATION

This thesis is dedicated to Bobby, Jessie, Mikey and Steven. Without your friendship and the many, many study sessions, I would not have survived these last four years.

ACKNOWLEDGEMENTS

From the absolute bottom of my heart, I would like to thank Dr. Kassab for all the opportunities he has offered me, and for his patient guidance, encouragement and advice that he has provided these last two years.

I would like to also thank Kyle Beggs for his wit and guidance while using Star-CCM+. Without his help, I would have never seen results.

I would also like to express a special thank you to my parents, Bruce and Elaine Ashley. Through your endless support and loving sacrifice, all of this was possible.

TABLE OF CONTENTS

LIST OF FIGURES

LIST OF TABLES

LIST OF ACRONYMS

POD	Proper orthogonal decomposition
RBF	Radial basis function
CFD	Computational fluid dynamics
$\boldsymbol{u}$	Snapshot vector
$\boldsymbol{p}$	Vector of parameters
$\boldsymbol{U}$	Snapshot matrix
f	Arbitrary functions
M	Number of snapshots
N	Number of nodes
K	Truncation point
$\boldsymbol{\Phi}$	Basis functions/vectors
A	Amplitudes matrix
$\boldsymbol{C}$	Covariance matrix
$\boldsymbol{V}$	Eigenvectors of *C*
λ	Eigenvalues
Λ	Matrix of eigenvalues
B	Matrix of interpolation coefficients
F	Matrix of interpolation functions
$f(p)$	Hardy inverse multi-quadric RBF
c	RBF smoothing constant

CHAPTER 1 – INTRODUCTION

The concept of proper orthogonal decomposition (POD) was developed about 100 years ago as a tool for processing statistical data [1]. Several techniques have previously been developed to solve *direct problems* (those defined as solutions with a complete set of input data, where all system parameters are known), but it is common in engineering to solve *inverse problems*, defined as ones where not all system-dependent parameters are known [2]. POD is a powerful, valuable technique with the ability to obtain low-dimensional approximate data of high dimensional processes. POD first captures a *snapshot* matrix which represents a collection of system measurements. It then generates a series of optimal basis functions that can best approximate the system. This optimality leads to excess error truncations, and in doing so, there is an enormous reduction in computation time [3]. “Essentially, POD removes unnecessary constraints that have little effect on the system as a whole” [3]. POD, in combination with a radial basis function (RBF) interpolation network which can determine interpolation coefficients, can accurately reproduce dimensional aspects, boundary conditions and/or material properties as they apply to the system or model [1].

As will be seen in this thesis, “POD – RBF has a natural ability for parameter estimation on its inverse characteristics. It can be applied to countless engineering applications that may have been tedious or laborious to solve otherwise” [3]. The full methodology of POD – RBF will be discussed in Chapter 3, and two important applications will be presented in Chapter 4. The first is a simple heat conduction problem which will train a POD model using RBFs over a set of sampled parameters used to compute the temperatures in a variable cross-section fin and subsequently to effectively predict the temperatures in that fin for specified parameter values that were not sampled

to build the POD. The second is a fluid mechanics problem involving the internal flow of a bifurcation modeling a vascular segment, which is meant to lay the ground work for future research in the optimization of a medical device for the heart – the left Ventricular Assist Device (LVAD).

Heart failure is one of the leading causes of death for men and women in the United States. Many conditions can damage or weaken the heart and, depending on the current or impending condition of the heart, there are options to consider for temporary and long-term solutions: by-pass surgery, heart transplant, or the assistance of medical devices [4]. In cases where donor compatibility is difficult to achieve, a Ventricular Assist Device (VAD) can be implemented to provide temporary circulatory support as a bridge to transplantation. While VADs are functionally capable and have been improved in design over the years, their efficiency depends upon the system's fluid composition and flow mechanics. Depending on the workload placed on the flow pump, pulsatile effects are almost entirely nullified, which is the major contributor to thrombo-embolism (stroke incidence) [5]. Still, the presence of this complication limits the widespread implementation of VAD therapy.

It is hypothesized that one way to reduce the risk of thrombo-embolism is to find an optimal angular displacement for the VAD, improving it further. Due to the complexity of this device in working conjunction with the cardiovascular system, it is necessary to understand its fundamental principles and to generate an accurate numerical model for further analysis. These underlying principles of the system include the material parameters, the boundary conditions, and the defining dimensional characteristics. However, repeatedly solving the entire system while varying only one or two parameters can be a long, tedious and expensive process. It is proposed that applying POD – RBF can provide the model reduction, error filtration and regularization to solve and optimize

the LVAD without accumulating extensive computation time. The bifurcation problem defined and solved in Chapter 4 is the first step in preparing and improving the LVAD system.

CHAPTER 2 – BACKGROUND

The concept of proper orthogonal decomposition (POD) was developed about 100 years ago as a statistical tool for processing and correlating data [3]. Over the years it has been implemented in applications of signal processing, control theory, pattern recognition, data compression, and many others [6] – as well as parameter estimation, which is the focus of this thesis. POD has also been redeveloped, depending on how the input data is utilized. POD is known as singular value decomposition (SVD), principal component analysis (PCA) or Karhunen-Loéve decomposition (KLD). For the purpose of this thesis, we will only discuss POD.

The primary purpose of POD is to optimally choose the best way to correlate and model known data. POD does so by establishing a rotated coordinate system using the least number of coordinates required. For example, POD may reduce a three-dimensional coordinated frame into a two-dimensional one, if only minor variations are found in the third dimension [3]. To establish the rotate coordinate system, POD captures maximum projections of vectors (or data points) in the original frame. These vectors are said to be correlated if parallel to one another and uncorrelated if orthogonal (or perpendicular) to one another.

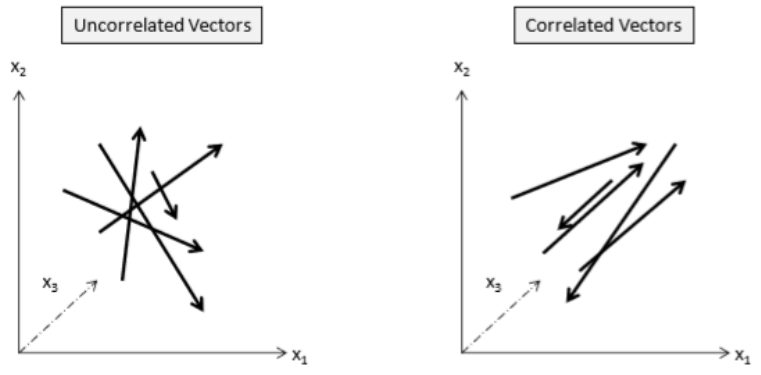

Figure 1: Illustration of uncorrelated (left) and correlated (right) vectors [3]

The first axis in the rotated POD frame grabs the maximum projections of the data from the original frame. The second axis captures the next largest projection and so on. This feature allows POD to more accurately approximate the vectors (or data points) with fewer coordinates.

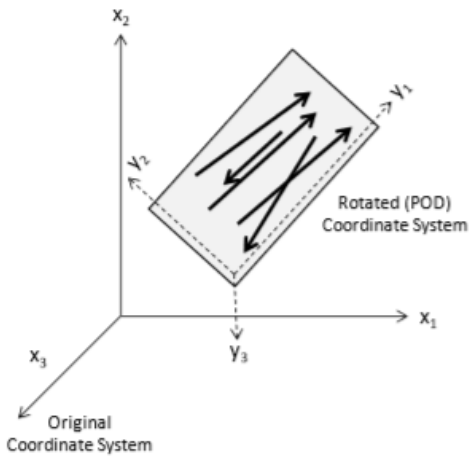

Figure 2: Original vs. rotated (POD) coordinate system

POD has been applied for modal analysis of data sets and in modal analysis of finite element methods to accelerate the solution process [8,9]. The concept of RBF trained POD has been useful to extend the application of POD to inverse problems and optimization [10], and this methodology is established in two important steps: (1) determine a truncated POD expansion of sampled data at sampled design parameters, and (2) interpolate the field using a trained RBF network for other desired parameter values. Chapter 3 will define these steps in detail.

CHAPTER 3 – METHODOLOGY

The POD provides a solution that takes advantage of the detail and accuracy of two- or three-dimensional computational fluid dynamics (CFD) analysis and calculates real-time parameters of various systems. To understand how POD – RBF can solve various applications, it is crucial to explain the discrete steps of implementing the technique.

The first step in the implementation of POD is the formation of the *snapshot*, which is the collection of sampled values of $\boldsymbol{u}$ based on parameter(s) $\boldsymbol{p}$. $\boldsymbol{u}$ refers to any kind of value recorded numerically or analytically – temperatures, velocities, reaction forces, and many others. By varying parameter(s) $\boldsymbol{p}$, a collection of M snapshot vectors, denoted as $\boldsymbol{u}^j$ (for j = 1, 2, … M), are then created and stored in a matrix called the *snapshot matrix*, denoted by $\boldsymbol{U}$ [3]. In the heat conductivity problem later described in Chapter 4, the snapshot matrix consists of sampled temperature fields and is obtained for assumed values of unknown parameters (in this case, varying heat conductivity and convective heat transfer coefficients). In general, the varied parameters can be any selection of boundary conditions or material parameters. Each $\boldsymbol{u}^j$ can then be stored and form a rectangular N by M matrix $\boldsymbol{U}$, denoted as the snapshot matrix [3].

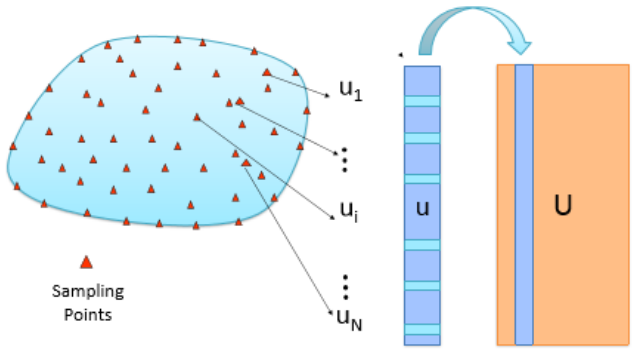

Figure 3: Illustration of a snapshot of the data field [3]

The snapshot matrix $\boldsymbol{U}$ is then used in POD to establish a set of orthonormal vectors $\boldsymbol{\Phi}^j$ (for j = 1, 2, … M) which should resemble the original matrix $\boldsymbol{U}$. The matrix $\boldsymbol{\Phi}$ is commonly referred to as the POD *basis* and can be defined as

$$\boldsymbol{\Phi} = \boldsymbol{U} \cdot \boldsymbol{V} \tag{1}$$

where $\boldsymbol{V}$ represents the eigenvectors of the covariance matrix $\boldsymbol{C}$ and is the nontrivial solution of the problem

$$\boldsymbol{C} \cdot \boldsymbol{V} = \boldsymbol{\Lambda} \cdot \boldsymbol{V}. \tag{2}$$

In the above equation, $\boldsymbol{\Lambda}$ is the diagonal matrix that stores eigenvalues λ of the symmetric, positive definite covariance matrix $\boldsymbol{C}$, which is defined as

$$\boldsymbol{C} = \boldsymbol{U}^{\boldsymbol{T}} \cdot \boldsymbol{U}. \tag{3}$$

Typically, λ is sorted in descending order and can often be attributed to the energy within the basis mode $\boldsymbol{\Phi}$. This energy decreases rapidly with increasing mode number, which allows the user to discard the majority of modes without influencing the accuracy of the representation. The resulting POD basis $\bar{\boldsymbol{\Phi}}$ is referred to as the *truncated* POD basis, consists of $K < M$ vectors, and is defined as (1). It is also known to be orthogonal $\boldsymbol{\Phi}^{\boldsymbol{T}} \cdot \boldsymbol{\Phi} = \boldsymbol{I}$ and presents the optimal approximation properties.

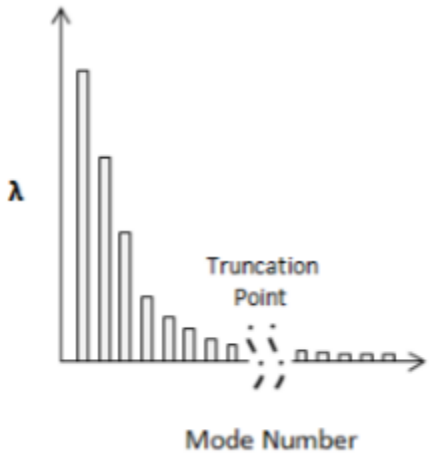

Figure 4: Truncation of eigenvalues for model reduction [3]

Once $\boldsymbol{\Phi}$ is known, the snapshot matrix $\boldsymbol{U}$ can be regenerated and approximated as

$$\boldsymbol{U} \cong \boldsymbol{\Phi} \cdot \boldsymbol{A} \tag{4}$$

where $\boldsymbol{A}$ represents the amplitudes associated with $\boldsymbol{u}^j$. These amplitudes can be computed from

$$\boldsymbol{A} = \boldsymbol{\Phi}^{\boldsymbol{T}} \cdot \boldsymbol{U}. \tag{5}$$

At this point, extrapolation of data can begin to determine information from the current problem. The amplitudes $\boldsymbol{A}$ are defined as

$$\boldsymbol{A} = \boldsymbol{B} \cdot \boldsymbol{F} \tag{6}$$

where matrix $\boldsymbol{B}$ contains the unknown constant coefficients of the current combination and $\boldsymbol{F}$ is the matrix of interpolation functions $f_j(\boldsymbol{p} - \boldsymbol{p}^j)$ chosen arbitrarily. However, since some choices could produce an ill-conditioned matrix $\boldsymbol{F}$, radial basis functions (RBFs) have been used for the purpose of this current research [6]. Employed is the Hardy inverse multi-quadric RBF, defined as

$$f_j(|\boldsymbol{p} - \boldsymbol{p}^j|) = \frac{1}{\sqrt{|\boldsymbol{p}-\boldsymbol{p}^j|^2+c^2}}, \tag{7}$$

where c stands for the smoothing factor. This parameter is chosen to "push the conditioning number of the RBF interpolation matrix $\boldsymbol{F}$, defined below, as high as numerically possible in order to obtain the highest interpolation from the RBF" [3].

$$\boldsymbol{F} = \begin{bmatrix} f_1(|\boldsymbol{p^1} - \boldsymbol{p}^1|) & \cdots & f_1(|\boldsymbol{p^j} - \boldsymbol{p}^1|) & \cdots & f_1(|\boldsymbol{p^M} - \boldsymbol{p}^1|) \\ \vdots & & \vdots & & \vdots \\ f_i(|\boldsymbol{p^1} - \boldsymbol{p}^i|) & \cdots & f_j(|\boldsymbol{p^j} - \boldsymbol{p}^i|) & \cdots & f_j(|\boldsymbol{p^M} - \boldsymbol{p}^i|) \\ \vdots & & \vdots & & \vdots \\ f_M(|\boldsymbol{p^1} - \boldsymbol{p}^M|) & \cdots & f_M(|\boldsymbol{p^j} - \boldsymbol{p}^M|) & \cdots & f_M(|\boldsymbol{p^M} - \boldsymbol{p}^M|) \end{bmatrix} \tag{8}$$

This is commonly referred to as collocation, where $\boldsymbol{p}^i$ and $\boldsymbol{p}^j$ are used to generate i^{th} or j^{th} snapshot respectively. The conditioning number of $\boldsymbol{F}$ is defined in a given matrix norm $\| \ \|$ as $K(\boldsymbol{F}) = \|\boldsymbol{F}\| \cdot \|\boldsymbol{F}^{-1}\|$. The sought-after coefficient matrix $\boldsymbol{B}$ can now be evaluated with a simple inversion

$$\boldsymbol{B} = \boldsymbol{A} \cdot \boldsymbol{F}^{-1}. \tag{9}$$

Now equating (5) and (6) yields

$$\boldsymbol{\Phi}^T \cdot \boldsymbol{U} = \boldsymbol{B} \cdot \boldsymbol{F}, \tag{10}$$

and using the orthogonality of $\boldsymbol{\Phi}$ the snapshot matrix $\boldsymbol{U}$ can be approximated as

$$\boldsymbol{U}(\boldsymbol{p}) \approx \boldsymbol{\Phi} \cdot \boldsymbol{B} \cdot \boldsymbol{F}. \tag{11}$$

This model will further be referred to as the *trained* POD – RBF network. The application of POD – RBF interpolation is capable of reducing the dimensionality of the model and reproducing the unknown field corresponding to any arbitrary set of parameters $\boldsymbol{p}$.

CHAPTER 4 – APPLICATIONS

The research objectives were: (1) to apply the fundamental principles of the POD – RBF approach in a verified Mathcad code, (2) train the method using a scalar heat conduction problem, (3) model a two-dimensional bifurcation, and (4) predict velocity values in the bifurcation given varying characteristic flow parameters. To satisfy these objectives, the investigation utilized the commercial computational fluid dynamics platform Star-CCM+ (Siemens, Melville, NY), engineering software Mathcad, and data collected from a series of numerical flow simulations.

The first application in Section 4.1 will cover objectives (1) and (2), outlining a basic heat conduction problem with a parabolic fin. Given a simple domain, the temperature values at specific locations along the fin were estimated using the POD – RBF model reduction technique.

In Section 4.2, objectives (3) and (4) are satisfied: the bifurcation was modeled and analyzed with POD – RBF in order to accurately predict velocity values given varying inlet mass flow rates. These estimated values are verified with numerical data obtained from Star-CCM+.

4.1 Fin Conduction Problem

To implement the fundamental principles of POD – RBF, a simple one-dimensional heat transfer problem was defined and solved using a second order accurate finite volume method to provide the data required to train the POD – RBF interpolation network. Using a parabolic fin, illustrated in Figure 5, an imposed uniform base temperature exchanges heat with its surroundings, and with the parameters listed in Table 1, the temperature values at eight nodes along the centerline were calculated using finite volume nodal equations. Then, using POD – RBF, the temperature

values at the same nodes were accurately predicted given different Biot numbers than those sampled to build the POD basis and train the POD – RBF.

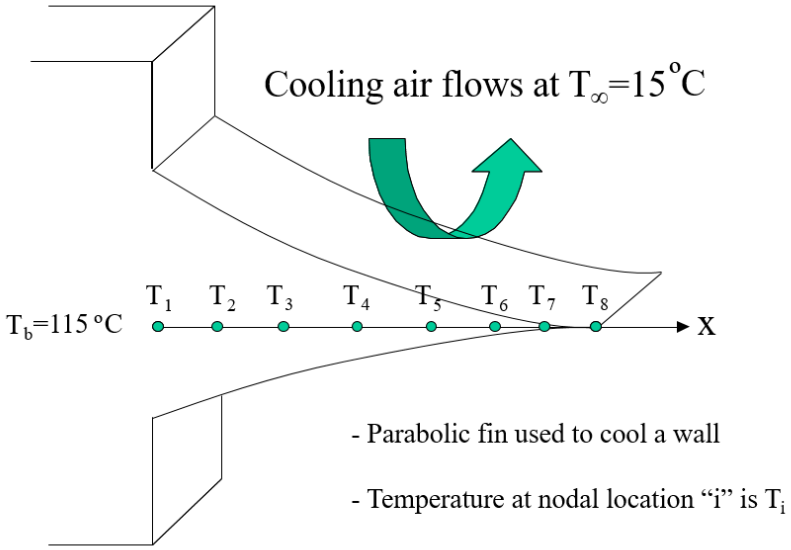

Geometric parameters

$L := 0.08$

$t := 0.016$

$x := 0, 0.001 .. 0.08$

Concave parabolic profile fin

$$yu(x) := \frac{t}{2}\cdot\left[\frac{(L - x)}{L}\right]^2$$

$$yl(x) := -yu(x)$$

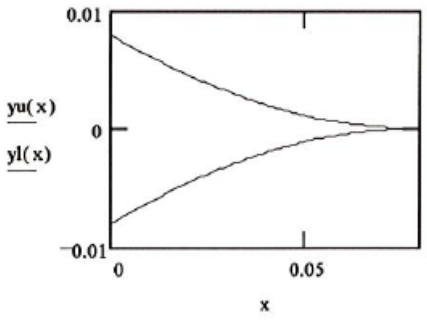

Figure 5: Parabolic fin

Fin Parameters	**Values**	**Units**
Step size (δ_x)	0.01	m
Length of fin (L)	0.08	m
Fin thickness (t)	0.016	m
Base temperature (T_b)	115	℃
Surrounding temperature (T_∞)	15	℃
Convection heat transfer coefficient (h)	100 200 500 800 1000	$\frac{W}{m^2 \cdot K}$
Thermal conductivity (k)	10 43 81 115 150	$\frac{W}{m \cdot K}$

Table 1: Fin dimensions and heat transfer properties

The general form of the energy equation for an extended surface under steady state conditions is

$$\frac{d^2T}{dx^2} + \left(\frac{1}{A_c}\frac{dA_c}{dx'}\right) - \frac{dT}{dx'} - \left(\frac{1}{A_c}\frac{h}{k}\frac{dA_s}{dx'}\right)(T - T_\infty) = 0 \tag{12}$$

where A_c is the horizontal confrontation of the differential element and x' is the length direction coordinate. This equation was discretized using the Finite Volume Method (FVM) based on second order central finite differences for the derivatives over $i = 1, 2 \ldots IL$ finite volumes. In this process arises a non-dimensional number, namely the Biot number that is a function of the convection coefficient ($\boldsymbol{h}$), the thermal conductivity ($\boldsymbol{k}$), and the l^{th} finite volume surface area per-unit length $\boldsymbol{\delta_l}$ given by

$$\boldsymbol{Bi} = \frac{\boldsymbol{h}}{\boldsymbol{k}} \cdot \boldsymbol{\delta_l} \tag{13}$$

where $\boldsymbol{Bi}$ denotes the Biot number. The finite volume nodal equations are as follows:

1. Left boundary finite volume ($i = 1$):

$$A_{i,i} = -2 \cdot \left[\left(\frac{y_A(i)}{\delta_x}\right) + \left(\frac{y_B(i)}{\delta_x}\right) + Bi_i\right]$$

$$A_{i,i+1} = 2 \cdot \frac{y_B(i)}{\delta_x}$$

$$b_i = -2 \cdot Bi_i \cdot T_\infty - 2 \cdot (\frac{y_A(i)}{\delta_x}) \cdot T_b$$

2. Interior finite volume ($2, 3 \ldots IL$):

$$A_{i,i} = -2 \cdot \left[\left(\frac{y_A(i)}{\delta_x}\right) + \left(\frac{y_B(i)}{\delta_x}\right) + Bi_i\right]$$

$$A_{i,i+1} = 2 \cdot \frac{y_B(i)}{\delta_x}$$

$$A_{i,i-1} = 2 \cdot \frac{y_A(i)}{\delta_x}$$

$$b_i = -2 \cdot Bi_i \cdot T_\infty$$

3. Right boundary finite volume ($i = IL$):

$$A_{i,i} = -\left[2 \cdot \left(\frac{y_A(i)}{\delta_x}\right) + (2 \cdot Bi)_i\right]$$

$$A_{i,i-1} = 2 \cdot \frac{y_A(i)}{\delta_x}$$

$$b_i = -(2 \cdot Bi)_i \cdot T_\infty$$

Here, $y_A(i)$ and $y_B(i)$ refer to the left and right control volume heights of the i^{th} finite volume respectively. These equations form a set of linear tridiagonal equations that are solved directly by the Thomas algorithm. The 25 Biot numbers corresponding to the sampled data span from $\boldsymbol{Bi} = 6.768 \times 10^{-3}$ to $\boldsymbol{Bi} = 1.015$ and these values are as follows:

$$\boldsymbol{Bi} = (0.102, 0.024, 0.013, 0.009, 0.007, 0.203, 0.047, 0.025, 0.018, 0.014, 0.508, 0.118, 0.063,$$

$$0.044, 0.034, 0.812, 0.189, 0.1, 0.071, 0.054, 1.015, 0.236, 0.125, 0.088, 0.068)$$

These relations were used to compute and establish the initial temperature matrix, referred to later during RBF extrapolation. For this problem, the Hardy inverse RBF interpolation equation can be defined as

$$\boldsymbol{f(Bi(h,k))} = \frac{\mathbf{1}}{\sqrt{\boldsymbol{Bi(h,k)^2 + c^2}}} \tag{14}$$

which was used to approximate the temperature values $\boldsymbol{u}$ along the fin.

$$\boldsymbol{U(h,k)} \approx \boldsymbol{\Phi \cdot B \cdot F(h,k)} \tag{15}$$

The temperature distributions (or the snapshot $N = 8$ long vector $\boldsymbol{u}$) was computed for all $M = 25$ variations of Biot numbers, and the $N \times M$ snapshot matrix $\boldsymbol{U}$ was generated. Performing POD on the covariance matrix $\boldsymbol{C}$ (3) generated eigenvalues shown in Figure 6 and could be truncated after the 7th term (out of a possible 16) listed in Table 2 [3].

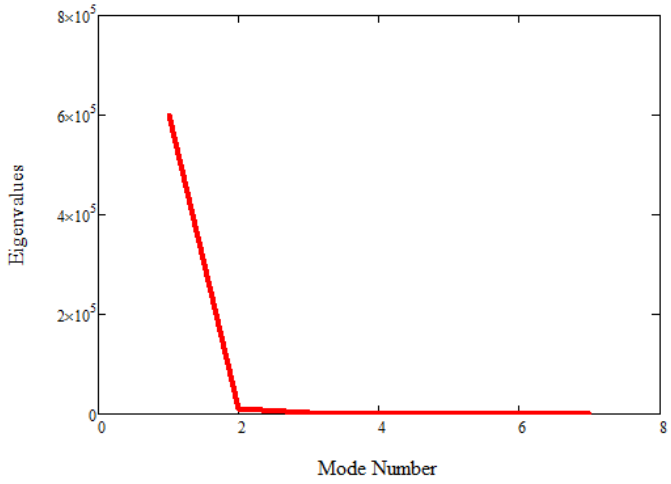

Figure 6: Plot of all eigenvalues for fin problem

$\boldsymbol{\lambda}$
$\mathbf{6.006 \times 10^5}$
$\mathbf{1.129 \times 10^4}$
$\mathbf{1.556 \times 10^3}$
$\mathbf{52.869}$
$\mathbf{11.388}$
$\mathbf{0.263}$
$\mathbf{0.012}$

Table 2: Truncated eigenvalues for fin problem

Truncating after 7 eigenvalues, a representative reconstruction of the FVM nodal temperatures for a Biot number $\boldsymbol{Bi} = 0.102$ is provided in Table 3. The error between the two vectors is 1.728×10^{-3} in the $L_\infty -$ norm.

Actual [℃]	**Approximation [℃]**
87.7328933	87.7329231
65.4117331	65.4115267
47.7170775	47.7177124
34.3101727	34.3091078
24.8213601	24.8223903
18.8299357	18.8293724
15.8216503	15.8218102
15.0481065	15.0480824

Table 3: Comparison of actual and POD – RBF approximation of temperature values for $Bi = 0.102$

An L_∞ (maximum) error or 1.236×10^{-4} is computed over all the sampled Biot numbers, which is highly accurate with only 7 eigenvalues utilized to estimate the system [3].

Now, the trained POD – RBF interpolation network can be used to accurately predict temperature values given non-sampled Biot numbers. 25 Biot numbers corresponding to the following convection coefficients and thermal conductivity values span from $\boldsymbol{Bi} = 6.924 \times 10^{-3}$ to $\boldsymbol{Bi} = 0.968$ and these values are as follows:

$$\boldsymbol{Bi} = (0.1, 0.024, 0.013, 0.009, 0.007, 0.192, 0.047, 0.025, 0.018, 0.013, 0.485, 0.118, 0.064,$$
$$0.044, 0.034, 0.772, 0.188, 0.101, 0.071, 0.054, 0.968, 0.235, 0.127, 0.088, 0.067)$$

Convection heat transfer coefficient (h)	103 199 501.5 798 1001	$\frac{W}{m^2 \cdot K}$
Thermal conductivity (k)	10.5 43.2 80 114.9 151	$\frac{W}{m \cdot K}$

Table 4: Non-sampled Biot numbers for fin problem

After interpolating the solution with the varied parameters, the temperature distribution along the fin was approximated. A representative reconstruction of the non-sampled nodal temperatures for a Biot number $\boldsymbol{Bi} = 0.192$ is provided in Table 5.

Approximation [℃]
78.238384
52.334218
35.075094
24.443267
18.610098
15.965068
15.122822
15.003932

Table 5: Interpolated temperature distribution along parabolic fin for $Bi = 0.192$

4.2 Bifurcation Problem

The following bifurcation application is a major stepping stone for the optimization of the left ventricular assist device (LVAD). It is proposed that modifying the angular displacement of the LVAD could improve its efficiency and functionality. However, repeatedly solving the entire system with only one or two parameters differing can be a long, tedious and expensive process. POD – RBF provides a reduced model approach to accurately predict desired parameters with little prior knowledge of the system. This simplified model was used to train the POD – RBF interpolation network for future investigation with the more complex system of the LVAD.

The two-dimensional *bifurcation* (one channel split into multiple channels) was modeled using the Star-CCM+ simulation platform and for the geometry shown in Figure 7.

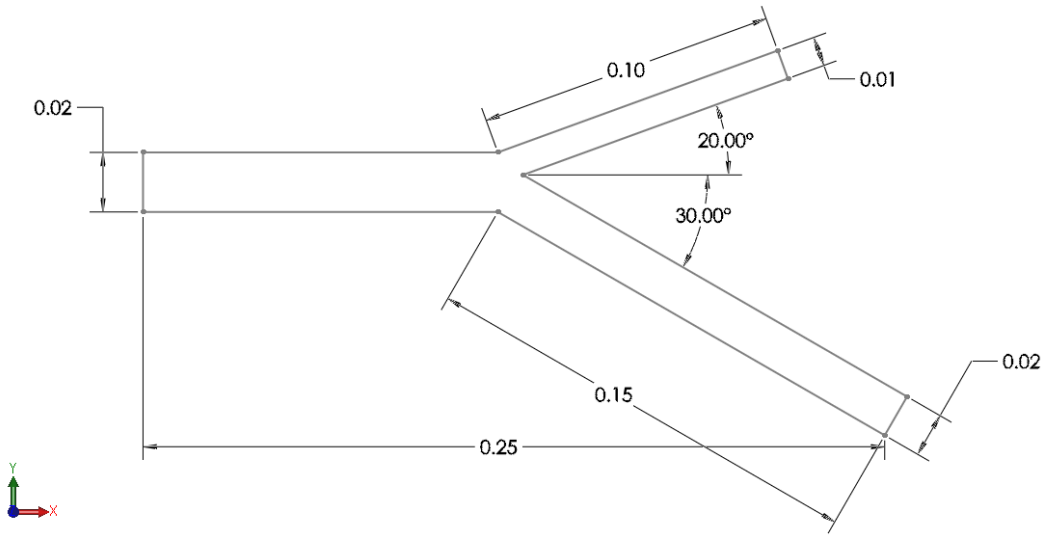

Figure 7: Geometry of bifurcation [m]

The flow is resolved by solving the Navier-Stokes equations

$$\nabla \cdot \vec{V} = 0 \tag{16}$$

$$\rho \frac{\partial \vec{V}}{\partial t} + \rho(\vec{V} \cdot \nabla)\vec{V} = -\nabla p + \mu \nabla^2 \vec{V} \tag{17}$$

in steady state for the velocity field $\vec{V}$ using the commercial CFD code Star-CCM+. The fluid domain is meshed using an unstructured mesh with the Star-CCM+ mesh generator ensuring proper grid density and a final mesh is established after a grid convergence study. Blood is modeled as a Newtonian incompressible fluid with density of $\rho = 1060\ kg/m^3$ and dynamic viscosity of $\mu = 0.0035\ \frac{N \cdot s}{m^2}$. The following parameters and initial and boundary conditions were applied to the bifurcation system:

Bifurcation Parameters	**Values**	**Units**
Mass flow rate ($\dot{m}$)	0.3	$\frac{kg}{s}$
Density (ρ)	1060	$\frac{kg}{m^3}$
Dynamic viscosity (μ)	0.0035	$Pa \cdot s$
Initial velocity (v)	0.01415	$\frac{m}{s}$
Reference pressure (P)	101325	Pa

Table 6: Bifurcation initial conditions

- No-slip on the fluid wall
- Laminar, steady and segregated flow solver with second order up-winding
- Varying mass flow rate (and consequently a varying initial velocity)
- Constant density, base size, dynamic viscosity, and reference pressure

A critical step for flow simulation is to generate a mesh for the system, which requires selection of the optimal base size for convergence and efficiency. For the most adept mesh, the base size will be large enough to converge but small enough to accurately gather data. After several iterations of the base size, the selected value was $0.8\ mm$. Figure 9 depicts the accuracy of velocity values taken at $70\ mm$ along the inlet channel (shown in Figure 8) given a varying base size. Figures 10 and 11 show the final generated mesh for the bifurcation and the associated converging residuals, respectively.

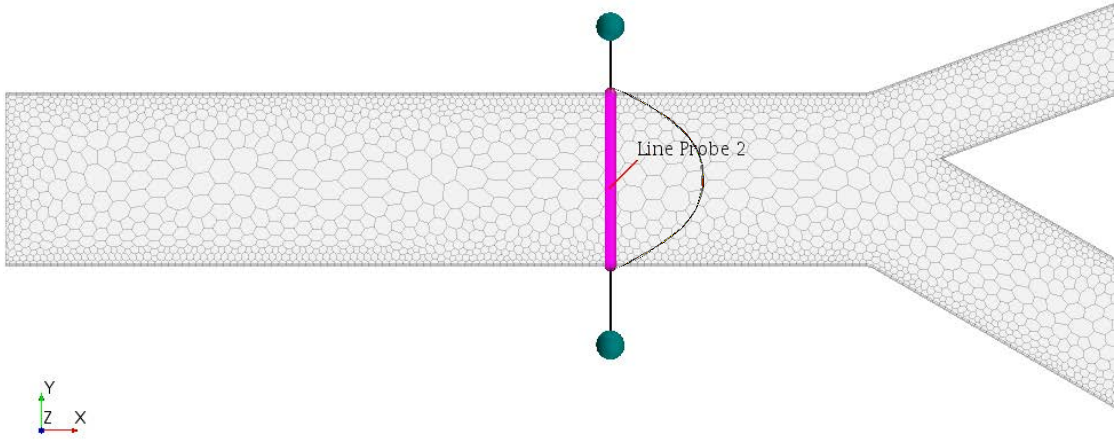

Figure 8: Location of sampled cross-section for mesh convergence

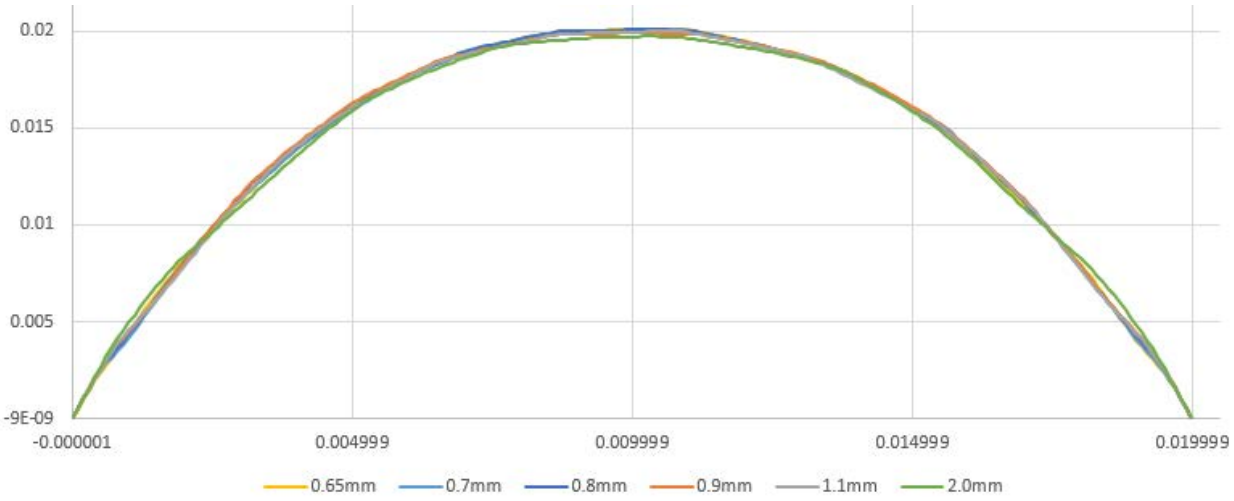

Figure 9: Mesh convergence: comparison of velocity values computed with varying base size

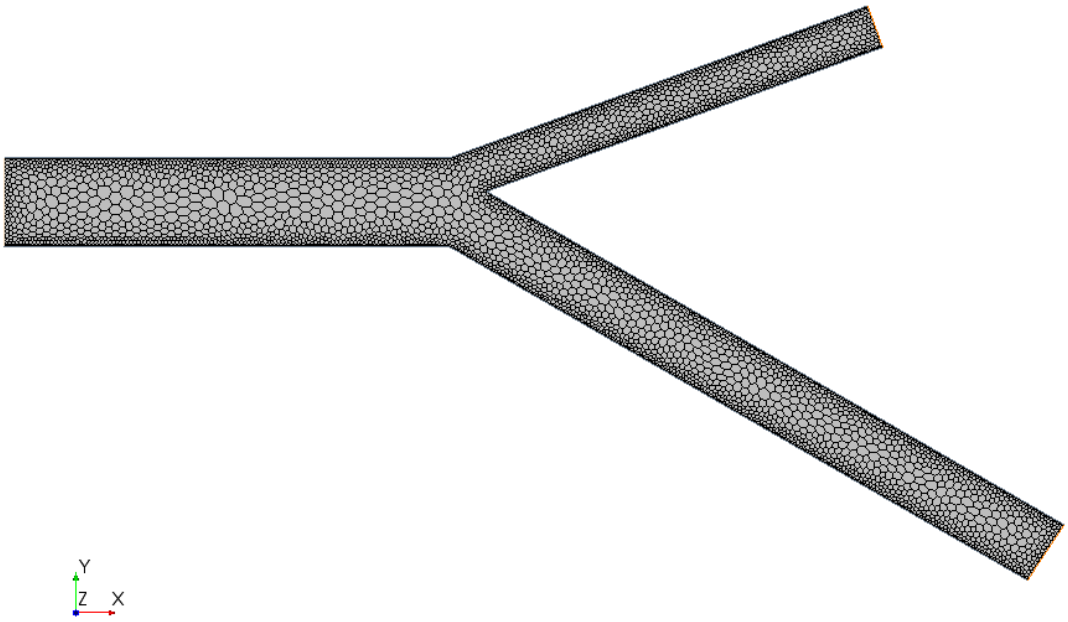

Figure 10: Bifurcation mesh

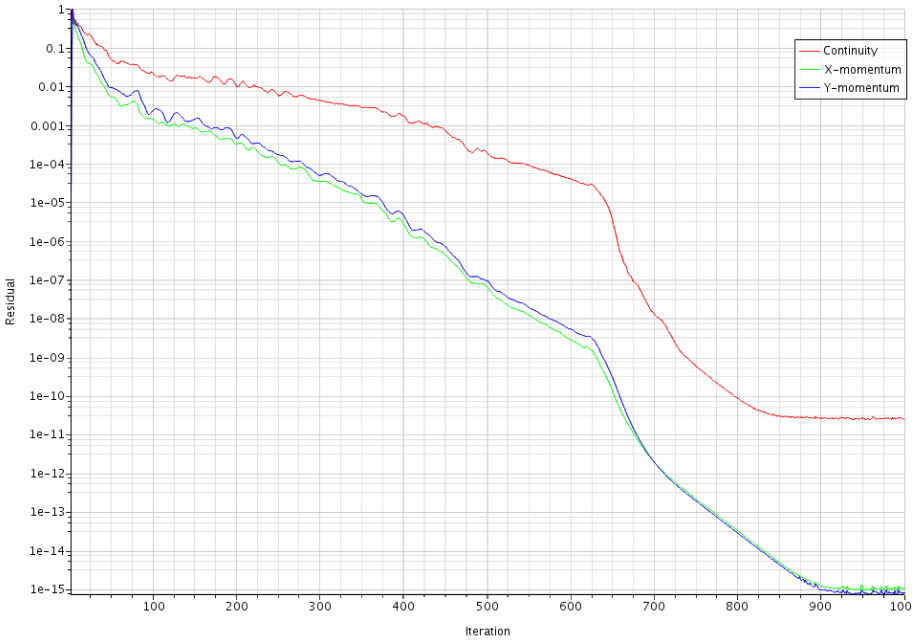

Figure 11: Residuals for bifurcation ($\dot{m} = 0.3\ kg/s$ and $b = 0.8\ mm$)

Once the converged mesh was generated, flow simulations were executed to measure and analyze the velocity profiles at various locations along the bifurcation.

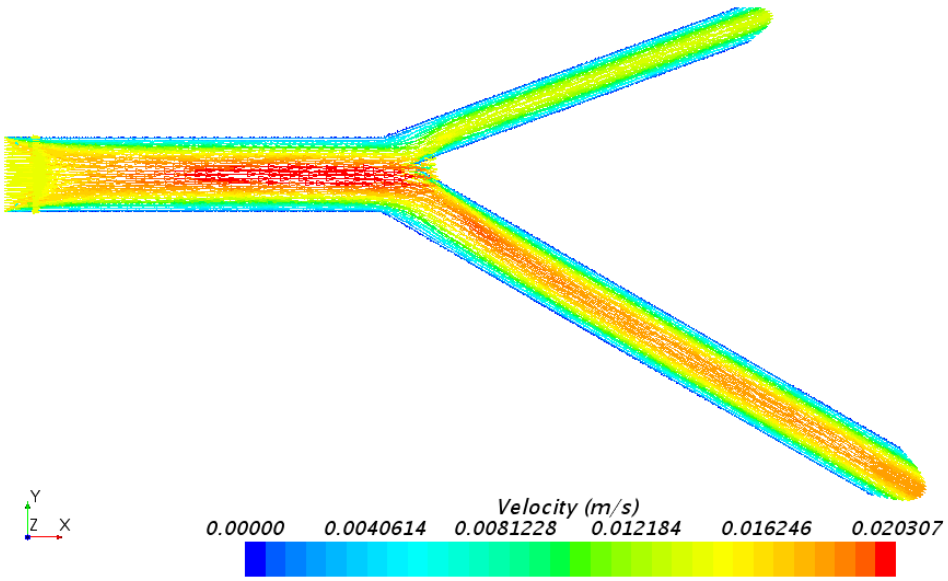

Figure 12: Velocity profile along bifurcation

The first step in the implementation of POD – RBF is the formation of the snapshot matrix. Velocity values computed at the specific and significant locations displayed in Figure 13 were exported into Mathcad and used as the collection of snapshots. There were 200 points in each cross-section for 7 cross-sections leading to N = 1400 long snapshot vectors of the velocity magnitude. The inlet mass flow rate was varied over the range of $0.2\,kg/s$ to $0.25\,kg/s$ to generate the POD data set.

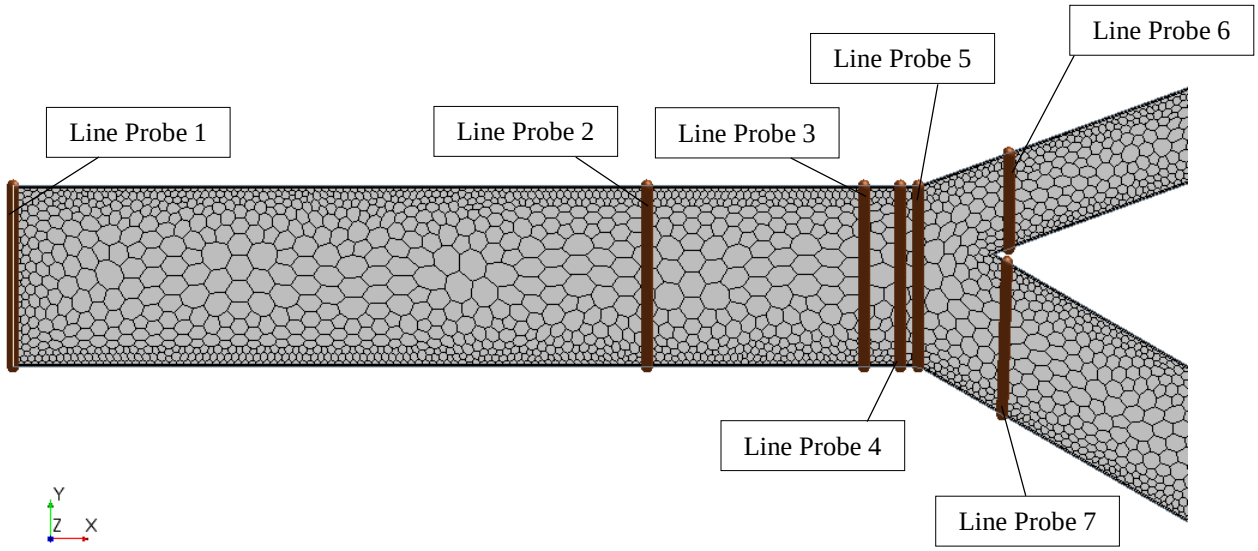

Figure 13: Location of sampled cross-sections for bifurcation problem

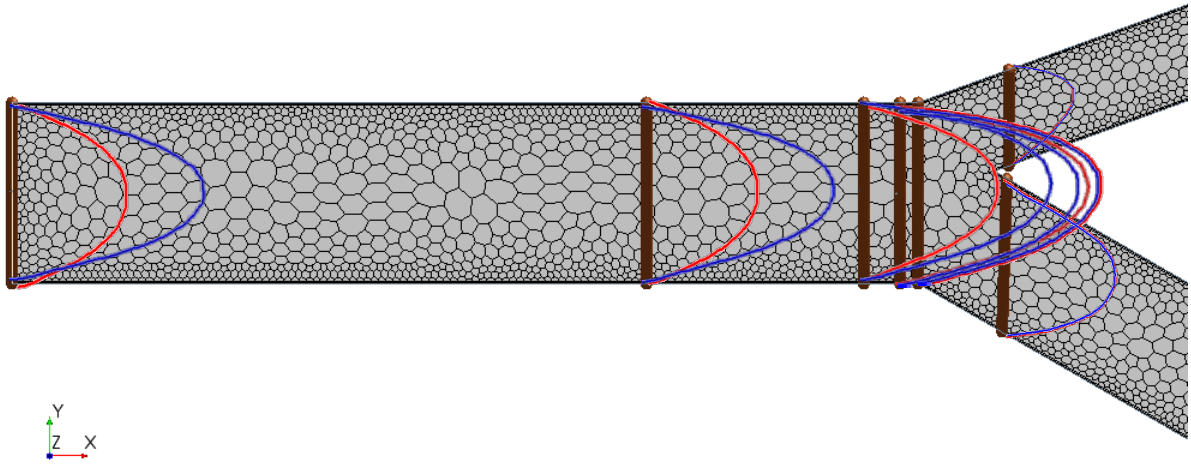

Figure 14: Velocity profiles for $\dot{m} = 0.2\ kg/s$ (red) and $\dot{m} = 0.25\ kg/s$ (blue) at cross-sections (Figure 13)

Performing POD on the covariance matrix $\boldsymbol{C}$ (3) generated eigenvalues shown in Figure 15 and can be truncated after the 6th term (out of the possible 10) listed in Table 7.

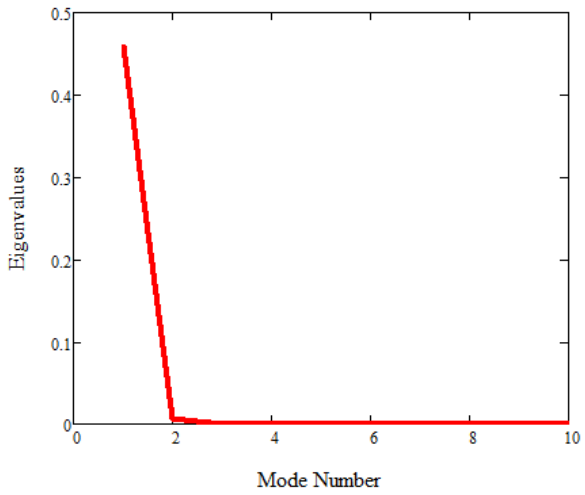

Figure 15: Plot of all eigenvalues for bifurcation problem

λ
0.458906
7.2239×10^{-3}
1.10128×10^{-4}
1.63558×10^{-5}
1.80197×10^{-6}
1.09426×10^{-6}

Table 7: Truncated eigenvalues for bifurcation problem

Performing the subsequent steps in the POD – RBF interpolation network gives an accurate approximation for velocity values along the bifurcation given a varying mass flow rate.

Actual [m/s]	Approximation [m/s]
0	-0.000000019903
0.000599899544	0.00059987248
0.00121431368	0.0012142684
0.00183481506	0.00183476764
0.00246429658	0.00246424112
0.00317396665	0.003173896373
0.003486347018	0.00348626266
0.003872970682	0.0038728761574

Table 8: Comparison of actual and POD – RBF approximation of velocity values ($\dot{m} = 0.2\ kg/s$)

For a non-sampled mass flow rate of $0.3\ kg/s$, the first eight velocity values in the cross-section at Line Probe 3 (Figure 14) are listed in Table 9. When later compared with evaluated velocity values at the same inlet mass flow rate, the maximum error was 7.054×10^{-8}, which is highly accurate using only 6 eigenvalues to estimate the velocity profiles.

Approximation [m/s]
0
0.0005999002543
0.00121431501827
0.0018348169993
0.0024642991033
0.00317396981327
0.00348635044926
0.00387297444039

Table 9: Velocity values at non-sampled mass flow rate ($\dot{m} = 0.3\ kg/s$)

CHAPTER 5 – DISCUSSIONS

The POD – RBF inverse approach proposed and implemented in this thesis provided an accurate parameter estimation of desired system values, even when few material characteristics or boundary conditions were known about the system. As shown in the examples solved in Chapter 4, POD needs only a few eigenvalues from the initial parameter snapshot matrix to estimate the desired solution, and RBF can interpolate the solution for new values of parameter(s) $\boldsymbol{p}$. RBF – trained POD serves as an inexpensive and efficient method of optimizing the accuracy of parameters or characteristics to be determined without accumulating extensive computation time.

With respect to the bifurcation, this thesis shows that the POD – RBF inverse approach can be applied for the optimization of the LVAD – a much more complicated system and domain. Since this technique can reduce the degrees of freedom in the system, the desired solution, given its varying parameters, can converge quickly and effortlessly with the implementation of this interpolation network.

REFERENCES

[1] Pearson, K. (1901). Of lines and planes of closest fit to system of points in space. The London, Edinburgh and Dublin Philosophical Magazine and Journal of Science, 2, 559-572.

[2] Ostrowski, Z., Bialecki, R.A. and Kassab, A.J., "Estimation of constant thermal conductivity by use of Proper Orthogonal Decomposition," Computational Mechanics, Vol. 37, No. 1, 2005, pp. 52-59.

[3] Rogers, C. (2010). Parameter estimation in heat transfer and elasticity using trained POD-RBF network inverse methods, UCF MS Thesis, 2010.

[4] Prather, R. (2015). A multi-scale CFD analysis of patient-specific geometries to tailor LVAD cannula implantation under pulsatile flow conditions: an investigation aimed at reducing stroke incidence in LVADs.

[5] Prather, R. O., Kassab, A., Ni, M. W., Divo, E., Argueta-Morales, R., & DeCampli, W. M. (2017). Multi-scale pulsatile CFD modeling of thrombus transport in a patient-specific LVAD implantation. *International Journal of Numerical Methods for Heat & Fluid Flow*, *27*(5), 1022-1039.

[6] Buljak, V. (2010). Proper orthogonal decomposition and radial basis functions algorithm for diagnostic procedure based on inverse analysis. *FME Transactions*, *38*(3), 129-136.

[7] Rogers, C. A., Kassab, A. J., Divo, E. A., Ostrowski, Z., & Bialecki, R. A. (2012). An inverse POD-RBF network approach to parameter estimation in mechanics. *Inverse Problems in Science and Engineering*, *20*(5), 749-767.

[8] Fic, A., Bialecki, R., and Kassab, A., "Solving Transient Non-linear Heat Conduction Problems by Proper Orthogonal Decomposition and FEM," Numerical Heat Transfer, Part A, Fundamentals, Vol. 48, No. 2, 2005, pp. 103-124.

[9] Bialecki, R.A., Kassab, A.J., and Fic, A, "Proper Orthogonal Decomposition and Modal Analysis for Acceleration of Transient FEM Models," International Journal for Numerical Methods in Engineering, Vol. 62, 2005, pp. 774-797.

[10] Huayamave, V., Ceballos, A., Barriento, C., Seigneur, H., Barkaszi, S., Divo, A., and Kassab, A., "RBF-Trained POD-Accelerated CFD Analysis of Wind Loads on PV systems," International Journal of Numerical Methods for Heat and Fluid Flow, 2017, Vol 27, No. 3, pp. 660-673.